Enhanced Orbital Magnetism in $Fe_{50}Pt_{50}$ Nanoparticles

C. Antoniak, J. Lindner, M. Spasova, D. Sudfeld, M. Acet, and M. Farle
Experimentalphysik—AG Farle, Fachbereich Physik, Universität Duisburg-Essen, Lotharstrasse 1, 47048 Duisburg, Germany

K. Fauth
Experimentelle Physik IV, Universität Würzburg, Am Hubland, 97074 Würzburg, Germany, and MPI für Metallforschung, Heisenbergstrasse 3, 70569 Stuttgart, Germany

U. Wiedwald, H.-G. Boyen, and P. Ziemann
Abteilung Festkörperphysik, Universität Ulm, Albert-Einstein-Allee 11, 89069 Ulm, Germany

F. Wilhelm and A. Rogalev
European Synchrotron Radiation Facility (ESRF), 6 Rue Jules Horowitz, BP 220, 38043 Grenoble Cedex, France

Shouheng Sun
Department of Chemistry, Brown University, Providence, Rhode Island 02912, USA
(Received 28 September 2005; published 13 September 2006)

X-ray absorption and magnetic circular dichroism spectra at both the Fe and Pt $L_{3,2}$ edges were measured on wet-chemically synthesized monodisperse $Fe_{50}Pt_{50}$ particles with a mean diameter of 6.3 nm before and after complete removal of the organic ligands and the oxide shell covering the particles by soft hydrogen plasma resulting in a pure metallic state. After thermal treatment of the metallic particles, the coercive field increased by a factor of 6, the orbital magnetic moment at the Fe site increased by 330% and is reduced at the Pt site by 30%, while the effective spin moments did not change. A decrease of the frequency of oscillations in the extended x-ray absorption fine structure at the Pt $L_{3,2}$ edges provides evidence for crystallographic changes towards the $L1_0$ phase.

DOI: 10.1103/PhysRevLett.97.117201 PACS numbers: 75.75.+a, 61.10.Ht, 61.46.−w, 78.70.Dm

The magnetic properties of nanoparticles with diameters <7 nm may differ from those of the corresponding bulk materials due to finite size effects, different crystal structures, and large surface contributions. Microscopic quantities like the orbital and spin magnetic moments are expected to reflect changes in crystal and electronic structure in a very sensitive way. In the case of bimetallic alloys like FePt, also the differences in composition at the surface and in the volume may lead to characteristic changes of the magnetic moments in Fe and Pt in a nanoparticle. From the technological perspective, FePt has become one of the most intensely researched nanostructured materials (see, e.g., [1–6]), since its large magnetic anisotropy of $K_{\mathrm{eff}} = 6 \times 10^6$ J/m^3 [7,8] and associated large coercivity makes it the prime candidate for new ultrahigh density magnetic storage media or biomedical applications [6]. Organometallic synthesis of FePt nanoparticles with subsequent heat treatment has been tried as an inexpensive route to obtain $L1_0$ ordered FePt particles with diameters around 4 nm [7]. Later analysis, however, has unambiguously shown that the thermal treatment led to agglomerated large crystals [9]. Here, we focus on the determination of the Fe and Pt magnetic moments in nonagglomerated wet-chemically synthesized FePt particles. The changes from the as prepared ligand covered state, over the pure metallic chemically disordered fcc state without a ligand shell, to a partially chemically ordered fct state after annealing are examined. At all stages the size distribution of the particles was monitored by high-resolution scanning electron microscopy (SEM). Specifically, we demonstrate the following: (i) pure metallic 6 nm $Fe_{50}Pt_{50}$ particles self-assembled on a Si wafer can be derived from the wet-chemical synthesis after a soft hydrogen plasma treatment; (ii) subsequent annealing at 600 °C yields structurally modified nanoparticles and a dramatic enhancement (330%) of the orbital magnetic moment μ_l at the Fe site while μ_l at the Pt site is slightly reduced and the effective spin magnetic moments remain unchanged after annealing; (iii) the structural transformation after annealing is evidenced by the lower frequency of the extended x-ray absorption fine structure (EXAFS) oscillations. In addition, the increase of the coercive field after thermal treatment indicates the partial formation of the chemically ordered $L1_0$ state.

The as prepared sample consists of monodisperse nanoparticles with a mean diameter of $d = 6.3$ nm and a standard deviation of $\sigma = 0.9$ nm of a chemically disordered $Fe_{50}Pt_{50}$ alloy surrounded by a ligand shell of oleyl amine and oleic acid. The particles, suspended in hexane, were deposited by spin coating onto a naturally oxidized Si substrate to form a monolayer. SEM images show a coverage of 10% on a 5×10 mm^2 area and the formation of

monolayer islands of about 2×10^4 nm^2 consisting of hexagonally arranged particles with a mean center-to-center distance $d_{cc} \approx 9$ nm.

For the determination of the element specific magnetic moments, x-ray absorption spectroscopy (XAS) spectra of the identical sample of photon energy were taken at the Fe $L_{3,2}$ and Pt $L_{3,2}$ edges in the total electron yield (TEY) mode at the PM-3 bending magnet beam line of the BESSY II synchrotron facility in Berlin, Germany, in fields of ± 2.8 T and in the hard x-ray regime in the fluorescence yield mode at the undulator beam line ID12 of the ESRF in Grenoble, France, in fields of ± 0.6 T. After each scan, either the magnetic field or the polarization of the x rays was flipped.

Figure 1 shows the normalized XAS, the corresponding x-ray magnetic circular dichroism (XMCD), and the integrated XMCD signal at the Fe and Pt $L_{3,2}$ edges in the hydrogen plasma treated and annealed states of the particles. To separate the electron excitations to unoccupied d states from those to the continuum, a standard two-step-like function is subtracted in the case of the spectra at the Fe $L_{3,2}$ edges [10]. Since the error in performing such a separation for the Pt $L_{3,2}$ edges is large due to the not well pronounced absorption peaks, the adjusted isotropic absorption spectra of Au were subtracted instead [11]. The XAS of the sample in the as prepared state at the Fe $L_{3,2}$ edges showed that the ligand shell does not protect the surface of the particles from oxidation, confirming previous results [12,13]. After the sample was exposed to a soft hydrogen plasma at room temperature and a pressure of 5 Pa, pure metallic XAS at the Fe $L_{3,2}$ edges was obtained [Fig. 1(a)]. At the carbon K edge, no absorption peaks were observed, since the hydrogen plasma does not only reduce Fe oxides but also removes the organic ligands as is also known for reactive oxygen plasma [14,15].

SEM images reveal that the number and the arrangement of particles have not changed within the error bars with respect to the as prepared state. In order to achieve the chemically ordered phase, the plasma treated particles have been annealed in hydrogen atmosphere of 5 Pa for 30 min at 600 °C. At this temperature the disorder-order transformation in FePt nanostructures takes place (see, e.g., [7,16–19]). Since the hard magnetic, chemically ordered $L1_0$ phase is known to have a large coercivity [13,20,21], element specific magnetization curves [22] at the Fe L_3 edge were measured to provide evidence for the formation of the $L1_0$ state. The normalized dichroic signal at $T = 15$ K as a function of the external magnetic field is shown for perpendicular and grazing incidence, i.e., for magnetization parallel to the normal of the sample plane ($\theta = 0°$) and $\theta = 75°$ (Fig. 2). The signals are normalized to the white line absorption. Before thermal treatment, the coercive field is $\mu_0 H_c = 36 \pm 5$ mT, and the magnetization is favored in plane due to weak dipolar interactions. After annealing, the coercive field is not only enhanced, but also found to depend slightly on the angle θ: $\mu_0 H_c(0°) = 292 \pm 8$ mT, $\mu_0 H_c(75°) = 228 \pm 8$ mT. Note that the sample may still not be fully saturated at $\mu_0 H = 2.8$ T for both geometries [Fig. 2(b)]. At 300 K, a clear hysteresis was observed with a coercive field of $\mu_0 H_c = 35 \pm 5$ mT. The values of the coercivity are in agreement to reported data for well-separated chemically ordered FePt particles of the same size with a random distribution of anisotropy axes [23] and are much smaller than the one for cosputtered FePt pancakelike particle layers for which a coercive field of 2 T at room temperature has been reported [8]. The ratio of remanence-to-saturation magnetization is 0.5, as predicted for randomly oriented, noninteracting particles by the Stoner-Wohlfarth theory, confirming that the dipolar coupling of the particles is negligible with respect to the large magnetocrystalline anisotropy of every single particle after annealing.

The size distribution obtained from a statistical analysis of many SEM images confirms that the median value of the diameter distribution does not change within the error bar

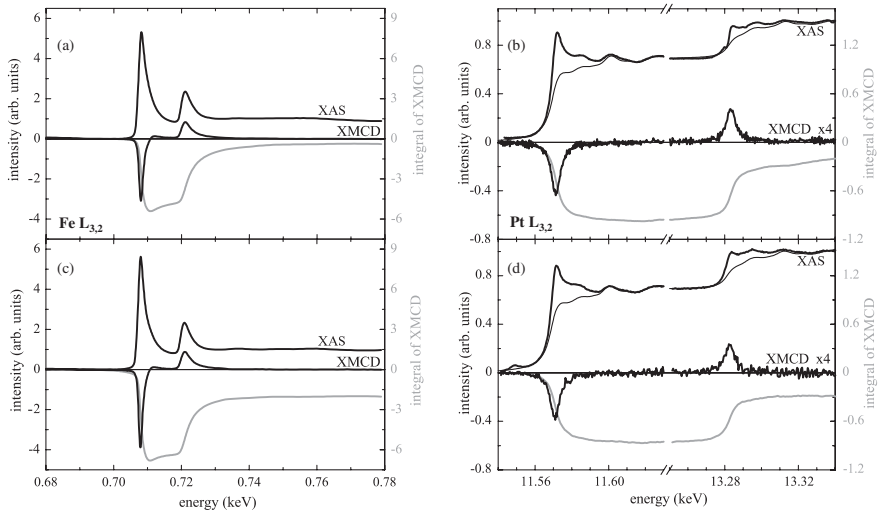

FIG. 1. Isotropic XAS, XMCD, and integrated XMCD spectra at 15 K for $Fe_{50}Pt_{50}$ nanoparticles after H plasma treatment (a),(b) and after annealing in H plasma (c),(d) measured at the Fe $L_{3,2}$ edges (left) and at the Pt $L_{3,2}$ edges (right). The thin lines in panels (b) and (d) are Au reference spectra with a shifted and stretched energy scale. XMCD spectra at the Pt $L_{3,2}$ edges are scaled up by a factor of 4.

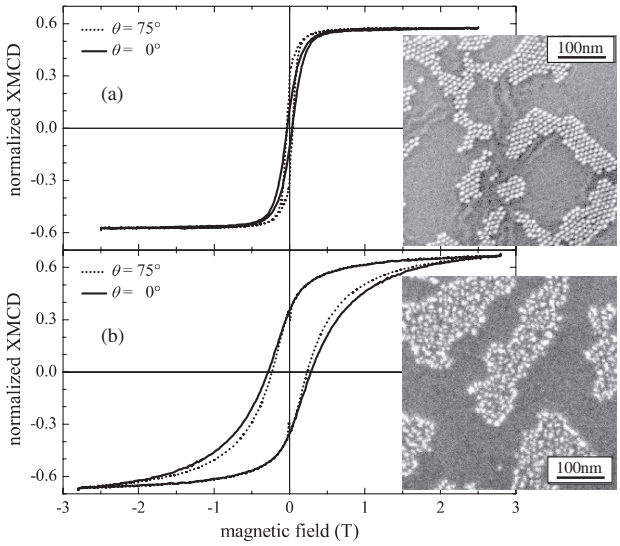

FIG. 2. Hysteresis loops of the XMCD for $Fe_{50}Pt_{50}$ nanoparticles at 15 K measured at the Fe L_3 edge for perpendicular ($\theta = 0°$, solid lines) and grazing ($\theta = 75°$, dotted lines) incidence (a) after H plasma treatment and (b) after 30 min annealing at 600 °C. The insets show SEM images of the sample before and after annealing.

and that more than 80% of the annealed sample consist of well-separated nanoparticles.

To address the question of whether structural distortions associated with the $L1_0$ phase occur, we analyzed the difference of the frequency of the EXAFS oscillations at the Pt $L_{3,2}$ edges of the metallic particles before and after annealing [Figs. 1(b) and 1(d)]. Using a Au reference spectrum, we determined a distance of nearest neighbor atoms consistent with the lattice constant of 3.85 ± 0.02 Å of the fcc disordered particles before annealing and a reduced one by $(2 \pm 1)\%$ after annealing in agreement to the corresponding decrease known in FePt bulk alloy [13,24].

By applying the XMCD sum rules [25] it is possible to determine the effective spin magnetic moment μ_s^{eff} and the orbital magnetic moment μ_l. $\mu_s^{\text{eff}} = \mu_s + 7\mu_t$ consists of the spin magnetic moment μ_s and the magnetic dipole moment μ_t which accounts for the asphericity of the spin moment distribution and might not cancel out especially in the case of nanostructured materials. Since the spin-orbit coupling in FePt is large, μ_t cannot be eliminated by angular dependent XMCD measurements [26], and even for randomly oriented crystallographic axes in the nanoparticle ensemble μ_t will not average out [27]. Hence, we can quote effective spin moments μ_s^{eff} only.

Values of μ_l and μ_s^{eff} obtained for Fe and Pt, which include a TEY saturation correction [28,29] of 3% for μ_s^{eff} and 30% for μ_l in the case of Fe moments, are listed in Table I. Absolute values were calculated using the theoretical numbers of d holes $\tilde{n}_h = n_h^{\text{Pt}} - n_h^{\text{Au}}$ with $n_h^{\text{Pt}} = 1.73$, $n_h^{\text{Au}} = 0.75$, and $n_h^{\text{Fe}} = 3.705$ [30] for both the disordered and the ordered states. Note that the different peak intensities in the XAS reveal a small decrease (<10%) of n_h^{Fe} after annealing, indicating a change in the electronic structure. The Pt moments of the annealed particles have been obtained by extrapolation to the saturation moments, since in the applied magnetic field of 0.6 T the XMCD is only about 74% of the one in the magnetically saturated state. For a better comparison, we also present in Table I the theoretical values (b) obtained from band structure calculations for a $L1_0$ structure and the values (a) derived from calculated XMCD spectra by application of the sum rules [30]. The later values include μ_t.

TABLE I. Element specific effective spin and orbital magnetic moments in μ_B. Theoretical values derived from band structure calculations (b) and from calculated XMCD spectra (a) for the $L1_0$ structure are also listed [30].

	Fe		Pt	
	μ_s^{eff}	μ_l	μ_s^{eff}	μ_l
Plasma treatment	2.48(25)	0.056(10)	0.41(2)	0.054(6)
Annealed	2.59(26)	0.240(18)	0.41(3)	0.042(6)
Theory (a)	2.50	0.064	0.41	0.020
Theory (b)	2.87	0.072	0.33	0.046

First, we discuss the spin moment of Fe and Pt. We found no significant change of μ_s^{eff} at both the Fe and Pt sites before and after annealing (Table I), in agreement to theory [31]. However, the absolute values of the spin moments at the Fe sites are about 15% smaller than the one obtained from band structure calculations ($2.87\mu_B$, [30,31]) for bulk materials. A reduction of the effective spin magnetic moment caused by a noncollinear spin structure at the particles surface [14] is assumed to be unlikely due to the dominating exchange energy between all spins in such small particles. One may note that for Fe nanoclusters a decrease of μ_s^{eff} with decreasing size was associated with a negative contribution of μ_t [32], which may be present in the FePt nanoparticles as well. Another reasonable explanation is the formation of small Fe clusters of a few atoms in the nonannealed particles resulting in a low-spin Fe state. In the case of Fe chains epitaxially grown at the steps of Pt(997) such a low-spin state was identified for a coverage above the monochain limit reflecting a strong dependence of μ_s^{eff} on the Fe-Fe coordination [33]. Additionally, in the case of the annealed particles the magnetic moments measured in 2.8 T may not be fully saturated (Fig. 2).

Now we turn to the discussion of the orbital contributions of the magnetic moments. At the Pt site, μ_l in the annealed particles is enhanced by about 100% compared to the calculated one for bulk. This is most likely due to the contribution of the increased orbital magnetic moments at the surface [34]. On the other hand, it is reduced by 30% with respect to the plasma treated (disordered) state. This may indicate local composition variations within the par-

ticle. One may argue that in the chemically disordered state a local segregation of a few atoms of Pt polarized by the Fe may effectively acquire a larger μ_l due to the larger spin-orbit coupling in Pt while μ_s remains the same. This effect may even be pronounced if the Pt enrichment occurs at the surface of the disordered particles. At the Fe site the orbital magnetic moment is strongly enhanced after annealing, namely, 330% with respect to the nonannealed state. The same dramatic increase is found when we consider just the ratio of orbital-to-spin magnetic moments, which is independent of the number of unoccupied d states. At the Fe site the ratio increases from 2% to 9% after annealing and is nearly identical to the ratio at the Pt site (10%) This indicates a noncubic environment of the Fe and Pt atoms as expected for the $L1_0$ structure.

In conclusion, we determined the element specific magnetic moments, μ_l and μ_s^{eff}, in pure metallic 6.3 nm $Fe_{50}Pt_{50}$ particles and found a strongly enhanced value of μ_l at the Fe site after annealing for 30 min at 600 °C. Evidence for local composition variations within the particles based on a comparison of all contributions to the magnetic moments is discussed. Additionally, changes of the EXAFS oscillations and the enhanced coercivity after thermal treatment indicate the partial formation of the $L1_0$ structure.

We thank A. Trounova, A. Schlachter, N. Friedenberger, and S. Stienen for assistance in the measurements. This work was supported by the BMBF (05 ES3XBA/5), the ESRF, the DFG (SFB 445, SFB 569, Zi 21-1), and the EU under Contract No. MRTN-CT-2004-005567 (SyntOrbMag).

[1] B. Rellinghaus, S. Stappert, M. Acet, and E. F. Wassermann, J. Magn. Magn. Mater. **266**, 142 (2003).
[2] R. W. Chantrell, D. Weller, T. J. Klemmer, S. Sun, and E. E. Fullerton, J. Appl. Phys. **91**, 6866 (2002).
[3] M. Ulmeanu, C. Antoniak, U. Wiedwald, M. Farle, Z. Frait, and S. Sun, Phys. Rev. B **69**, 054417 (2004).
[4] V. Sagueiriño-Maceira, L. M. Liz-Marzán, and M. Farle, Langmuir **20**, 6946 (2004).
[5] C. Antoniak, J. Lindner, and M. Farle, Europhys. Lett. **70**, 250 (2005).
[6] D. K. Kim, D. Kan, T. Veres, F. Normadin, J. K. Liao, H. H. Kim, S.-H. Lee, M. Zahn, and M. Muhammed, J. Appl. Phys. **97**, 10Q918 (2005).
[7] S. Sun, C. B. Murray, D. Weller, L. Folks, and A. Moser, Science **287**, 1989 (2000).
[8] T. Shima, K. Takanashi, Y. K. Takahashi, and K. Hono, Appl. Phys. Lett. **85**, 2571 (2004).
[9] H. Zeng, S. Sun, T. S. Vedanton, J. P. Liu, Z.-R. Dai, and Z.-L. Wang, Appl. Phys. Lett. **80**, 2583 (2002).
[10] C. T. Chen, Y. U. Idzerda, H.-J. Lin, N. V. Smith, G. Meigs, E. Chaban, G. H. Ho, E. Pellegrin, and F. Sette, Phys. Rev. Lett. **75**, 152 (1995).
[11] W. Grange, M. Maret, J.-P. Kappler, J. Vogel, A. Fontaine, F. Petroff, G. Krill, A. Rogalev, J. Goulon, M. Finazzi, and N. B. Brookes, Phys. Rev. B **58**, 6298 (1998).
[12] S. Anders, M. F. Toney, T. Thomson, J.-U. Thiele, B. D. Terris, S. Sun, and C. B. Murray, J. Appl. Phys. **93**, 7343 (2003).
[13] C. Liu, T. J. Klemmer, N. Shukla, X. Wu, D. Weller, M. Tanase, and D. Laughlin, J. Magn. Magn. Mater. **266**, 96 (2003).
[14] H.-G. Boyen, K. Fauth, B. Stahl, P. Ziemann, G. Kästle, F. Weigl, F. Banhart, M. Heßler, G. Schütz, N. S. Gajbhije, J. Ellrich, H. Hahn, M. Büttner, M. G. Garnier, and P. Oelhafen, Adv. Mater. **17**, 574 (2005).
[15] U. Wiedwald, K. Fauth, M. Heßler, H.-G. Boyen, F. Weigl, M. Hilgendorff, M. Giersig, G. Schütz, P. Ziemann, and M. Farle, Chem. Phys. Chem. **6**, 2522 (2005).
[16] Z. Jia, S. Kang, S. Shi, D. E. Nikles, and J. W. Harrell, J. Appl. Phys. **97**, 10J310 (2005).
[17] K. E. Elkins, T. S. Vedantam, J. P. Liu, H. Zeng, S. Sun, Y. Ding, and Z. L. Wang, Nano Lett. **3**, 1647 (2003).
[18] B. Bian, K. Sato, Y. Hirotsu, and A. Makino, Appl. Phys. Lett. **75**, 3686 (1999).
[19] Y. K. Takahashi, T. Koyama, M. Ohnuma, T. Ohkubo, and K. Hono, J. Appl. Phys. **95**, 2690 (2004).
[20] J. W. Harrell, S. Wang, D. E. Nikles, and M. Chen, Appl. Phys. Lett. **79**, 4393 (2001).
[21] B. Stahl, J. Ellrich, R. Theissmann, M. Ghafari, S. Bhattacharya, H. Hahn, N. S. Gajbhiye, D. Kramer, R. N. Viswanath, J. Weissmüller, and H. Gleiter, Phys. Rev. B **67**, 014422 (2003).
[22] E. Goering, A. Fuss, W. Weber, J. Will, and G. Schütz, J. Appl. Phys. **88**, 5920 (2000).
[23] J.-M. Qiu, J. H. Judy, D. Weller, and J.-P. Wang, J. Appl. Phys. **97**, 10J319 (2005).
[24] M. R. Visokay and R. Sinclair, Appl. Phys. Lett. **66**, 1692 (1995), and references therein.
[25] B. T. Thole, P. Carra, F. Sette, and G. van der Laan, Phys. Rev. Lett. **68**, 1943 (1992); P. Carra, B. T. Thole, M. Altarelli, and X. Wang, Phys. Rev. Lett. **70**, 694 (1993).
[26] J. Stöhr and H. König, Phys. Rev. Lett. **75**, 3748 (1995).
[27] C. Ederer, M. Komelj, and M. Fähnle, Phys. Rev. B **68**, 052402 (2003).
[28] R. Nakajima, J. Stöhr, and Y. U. Idzerda, Phys. Rev. B **59**, 6421 (1999).
[29] K. Fauth, Appl. Phys. Lett. **85**, 3271 (2004).
[30] I. Galanakis, M. Alouani, and H. Dreyssé, J. Magn. Magn. Mater. **242**, 27 (2002).
[31] Ya. Perlov, H. Ebert, A. N. Yaresko, V. N. Antonov, and D. Weller, Solid State Commun. **105**, 273 (1998).
[32] K. W. Edmonds, C. Binns, S. H. Baker, S. C. Thornton, C. Norris, J. B. Goedkoop, M. Finazzi, and N. B. Brookes, Phys. Rev. B **60**, 472 (1999).
[33] A. Enders (private communication).
[34] O. Šipr, M. Košuth, and H. Ebert, Phys. Rev. B **70**, 174423 (2004).